IJST, Transactions of Mechanical Engineering, Vol. 36, No. M1, pp 13-23
Printed in The Islamic Republic of Iran, 2012

MOLECULAR DYNAMICS SIMULATION OF MELTING, SOLIDIFICATION AND REMELTING PROCESSES OF ALUMINUM*

S. SOLHJOO,[1**] A. SIMCHI[2] AND H. AASHURI[2]

[1]Dept. of Materials Science and Engineering, School of Engineering, Shiraz University, I. R. of Iran
Email: soheilsolhjoo@yahoo.com
[1,2]Dept. of Material Science and Engineering, Sharif University of Technology, Tehran, I. R. of Iran

Abstract– A molecular dynamics simulation study has been performed to investigate the solidification and remelting of aluminum using Sutton-Chen many body potential. Different numbers of atoms from 108 to 2048 atoms were considered to find an adequate size for the system. Three different cooling and heating rates, i.e. 10^{12} K/s, 10^{13} K/s and 10^{14} K/s, were used. The structure of the system was examined using radial distribution function. The melting and crystallization temperatures of aluminum were evaluated by calculating the variation of heat capacity during the phase transformation. Additionally, Wendt–Abraham parameters were calculated to determine the glass transition temperature. It is shown that the melting temperature of aluminum increases as the heating rate increases. During solidification, a crystalline or amorphous-like structure is formed depending on the cooling rate. Remelting of the amorphous solidified material is accompanied by crystallization before melting at heating rates $<10^{14}$ K/s. The melting temperature also depends on the degree of structural crystallinity before remelting.

Keywords– Molecular dynamics, rapid solidification, remelting, metallic glasses, aluminum

1. INTRODUCTION

During rapid solidification of metals, amorphous and crystalline structures can be formed depending on the cooling rate. At high cooling rates, the crystallization may be suppressed and a metastable amorphous structure (metallic glass) is formed. Under such circumstances, the liquid structure with a short-range order is saved in the solid (amorphous) state. While the critical cooling rate for amorphization of conventional alloys is in the order of 10^6 K/s, the critical rate for pure metals is beyond 10^{12} K/s [1]. Studying the phase transition and nucleation phenomena in pure metals at such high cooling rates is not experimentally feasible. Molecular dynamics simulation is a very powerful tool that has been widely used in studying the crystallization and glass formation processes of metals during rapid solidification [2-22]. Since the cooling rates used in MD simulations are usually higher than the laboratory rapid quenching experiments, the MD results provide insight into the local structural features and the corresponding thermal dynamics properties under vigorous quenching conditions. In contrast to the solidification process of pure metals, literature review shows that the remelting of a rapid solidified liquid has been investigated limitedly. Pei et al. [8] reported remelting of Ti_3Al by MD simulation and reported a drop off in the internal energy during remelting due to crystallization of the amorphous solid. The aim of this work is to study the structural changes of aluminum during melting, freezing and remelting processes. The crystallization during cooling and heating processes was investigated and the effect of crystallinity on the remelting temperature was studied.

*Received by the editors October 27, 2011; Accepted February 29, 2012.
**Corresponding author

2. SIMULATION METHOD

An ISO/ANSI C++ standard code was developed to run equilibrium MD simulation in the canonical ensemble (NVT) with a constant number of atoms (N), volume (V) and temperature (T) with a time step of 0.1 fs. The periodic boundary conditions (PBC) were applied on the three dimensions of the MD cell. The weak coupling thermostat [23] was used to keep temperature constant at the specified set point. The equations of motion of the system were numerically solved using the velocity version of Verlet algorithm [24] with an integration step size of 10 fs.

In order to calculate the total cohesive energy of metallic bonding including many body interactions, Sutton-Chen potential [25] was used. The total potential energy of a metallic system (with finite atoms) is calculated from:

$$U_{total} = \sum_i \varepsilon \left[\frac{1}{2} \sum_{j \neq i} V(r_{ij}) - c\sqrt{\rho_i} \right] \tag{1}$$

$$V(r_{ij}) = \left(\frac{a}{r_{ij}} \right) \tag{2}$$

$$\rho_i = \sum_{j \neq i} \left(\frac{a}{r_{ij}} \right)^m \tag{3}$$

where r_{ij} is the distance between atoms i and j, ε a parameter with the dimensions of energy, c a positive dimensionless parameter, a a length parameter scaling all spacing (leading to dimensionless V and ρ) which is equal to lattice parameter, n and m are positive constants, $V(r_{ij})$ is the pair potential to account for the repulsion between the i and j atomic cores resulting from the Pauli's exclusion principle, and ρ_i the local density accounting for the cohesion associated with atom i. The potential parameters are obtained by fitting the experimental cohesive energies and lattice parameters. The potential parameters for aluminum are listed in Table 1 [26].

Table 1. Potential parameters of aluminum used in MD simulation [26]

m	n	ε (meV)	c	a (Å)
6	7	33.147	16.399	4.05

In order to choose adequate number of atoms, different systems with different number of atoms, i.e. 108, 256, 500, 864, 1372 and 2048, were considered for the melting process. These numbers of atoms were considered because of the simulation cell shape (cube) and the atomic structure of solid aluminum, which is fcc, in order to fill the whole cell. The simulation run was applied for 25 ps at 300 K for equilibration. Then, the temperature was gradually increased from 300 K to 1300 K with a heating rate of 10^{12} K/s. From the results (see 1st paragraph of "Results and discussion" section) a system containing 500 atoms was selected for the next steps.

In order to study melting, solidification and the remelting processes of aluminum, 500 atoms were considered. To attain equilibrium, the simulation run was applied for 25 ps at 300 K. The temperature was then gradually increased from 300 K to 1300 K at three different rates of 10^{12}, 10^{13} and 10^{14} K/s. At 1300 K the system was maintained for 5 ps and subsequently was cooled to 300 K at the same rate it was heated. After another relaxation time at 300 K for 5 ps, the temperature gradually increased up to 1300 K at the mentioned heating rates.

3. RESULTS AND DISCUSSION

The internal energy as a function of temperature during the heating process for the systems with different number of atoms is illustrated in Fig. 1. From the sudden changes in internal energy of systems which are related to the melting of the systems, the melting points are calculated (Table 2). As can be seen, the melting point lowered from 1060 K for 108 atoms to 940 K for 500 atoms. The melting point did not change for larger systems. Therefore, 500 atoms was considered for the next simulations. The reason for this temperature drop is based on the stability of the system; the system needs a minimum number of atoms to be stable. From a technical point of view, in MD simulations, smaller systems increase the energy in an unreasonable way.

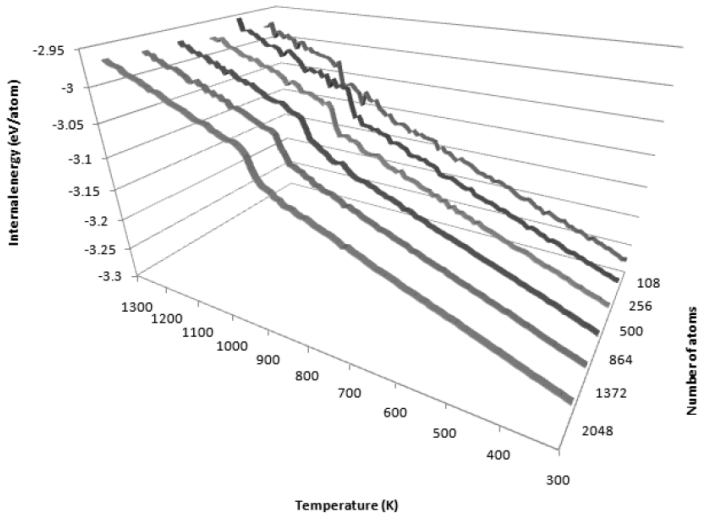

Fig. 1. Internal energy of the systems with different number of atoms as a function of temperature during the heating process with a rate of 10^{12} K/s

Table 2. Melting points (K) of aluminum from the systems with different number of atoms

No. of atoms	Melting temperature (K)
108	1060
256	970
500	940
864	940
1372	940
2048	940

Figure 2 shows the internal energy of the system as a function of temperature during heating of the system from 300 K to 1300 K. At the heating rate of 10^{12} K/s, a sudden increase in the internal energy in the temperature range of 896-907 K occurred. RDF results of this process are shown in Fig. 3a at some selected temperatures. In agreement with the internal energy variation, a change in the structure from crystalline to liquid can be seen at around 900 K, indicating melting of bulk aluminum. When the heating rate increased to 10^{13} K/s, the phase transformation temperature shifted to a higher temperature range of 942-958 K. Figure 2 also shows that this temperature range shifted and broadened, i.e. the change in the internal energy occurred gradually in the temperature range of 1100-1160 K for the heating rate of 10^{14} K/s. Figure 3b shows RDF results for this process at different temperatures. While at 1100 K a small fraction of crystalline structure was reserved, full liquid structure was obtained at 1200 K.

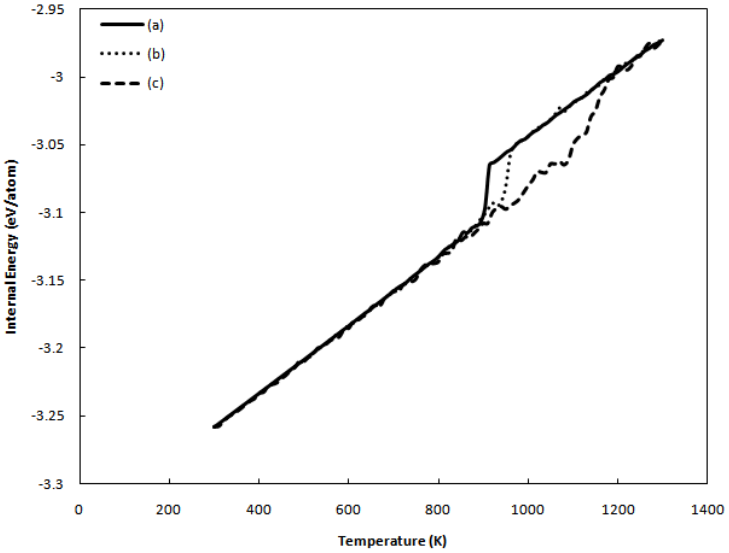

Fig. 2. Internal energy of the system as a function of temperature during heating at constant rate of (a) 10^{12} K/s, (b) 10^{13} K/s and (c) 10^{14} K/s

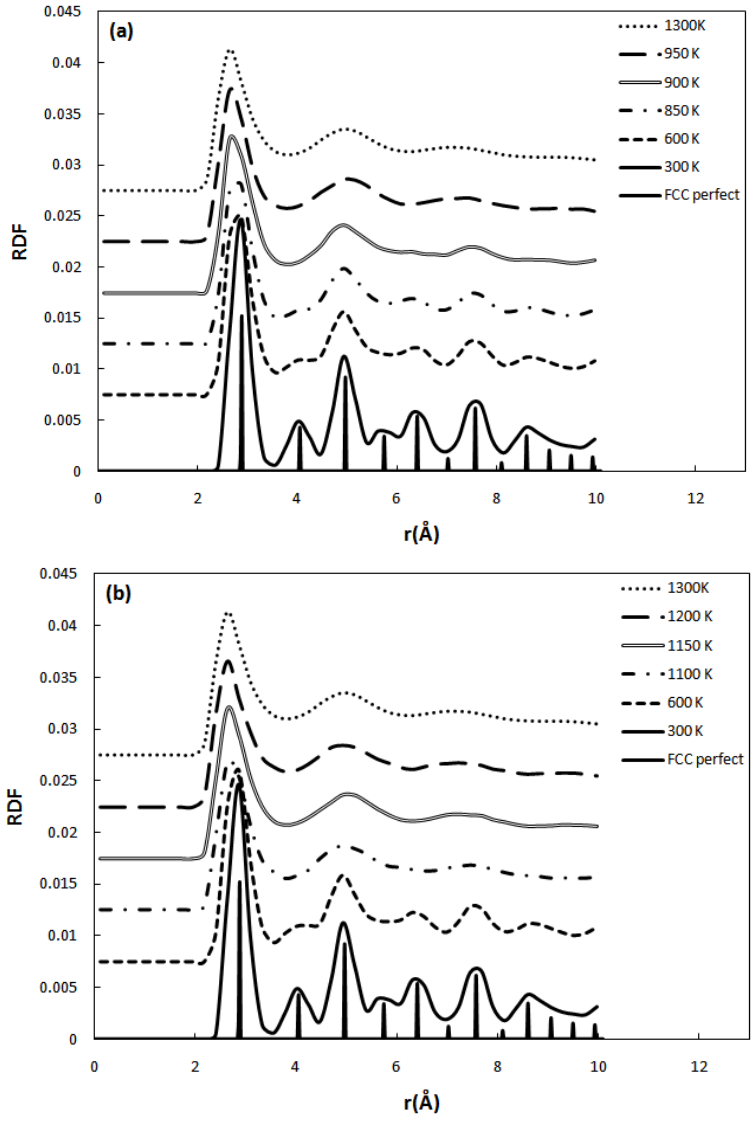

Fig. 3. Radial distribution function of aluminum at some selected temperatures: (a) 10^{12} K/s; (b) 10^{14} K/s

Figure 4 shows the internal energy of the system during the cooling process of the melted aluminum as a function of temperature depending on the freezing rate. Based on the variation of the internal energy, it appears that crystallization of the melt occurred at the cooling rate of 10^{12} K/s. The crystallization temperature was around 460 K. No crystallization was observed at higher cooling rates. Figure 5 shows the RDF of the rapidly solidified melts after relaxation for 5 ps at 300 K. In agreement with the internal energy variations (Fig. 4), an amorphous-like structure was obtained at $>10^{12}$ K/s. As shown in Fig. 6, increasing the relaxation time did not significantly change the result, i.e. the system had a little tendency to change its structure from amorphous-like to crystalline in the time up to 1 ns.

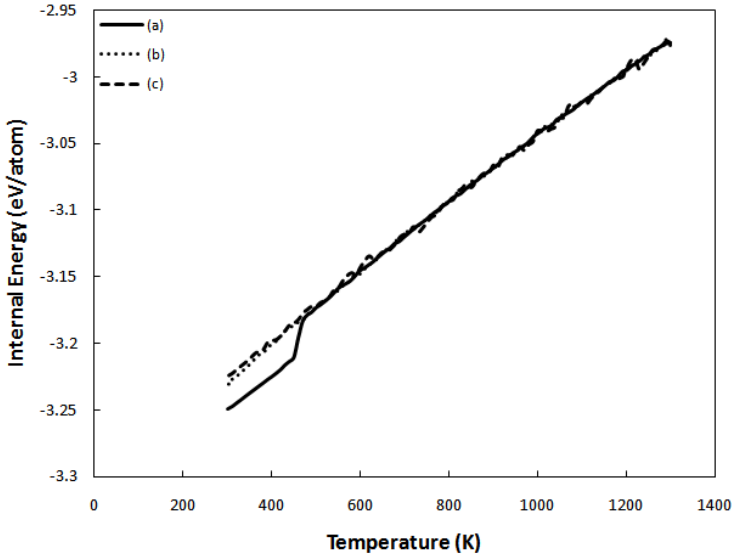

Fig. 4. Variation of internal energy vs. temperature during cooling process with rates of (a) 10^{12}K/s, (b) 10^{13}K/s and (c) 10^{14}K/s

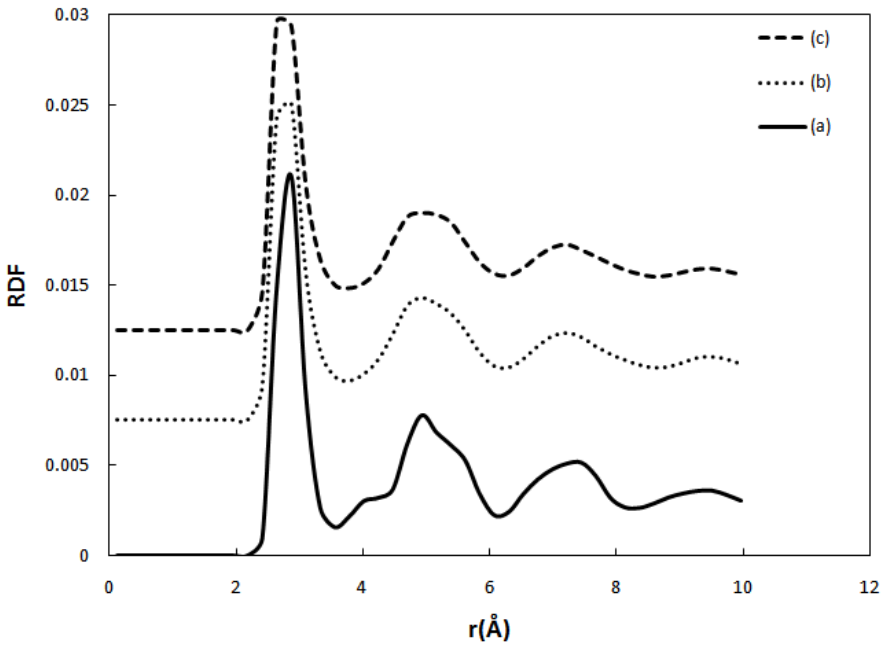

Fig. 5. RDF curves of rapidly solidified aluminum melt at a rate of (a) 10^{12} K/s, (b) 10^{13} K/s and (c) 10^{14} K/s

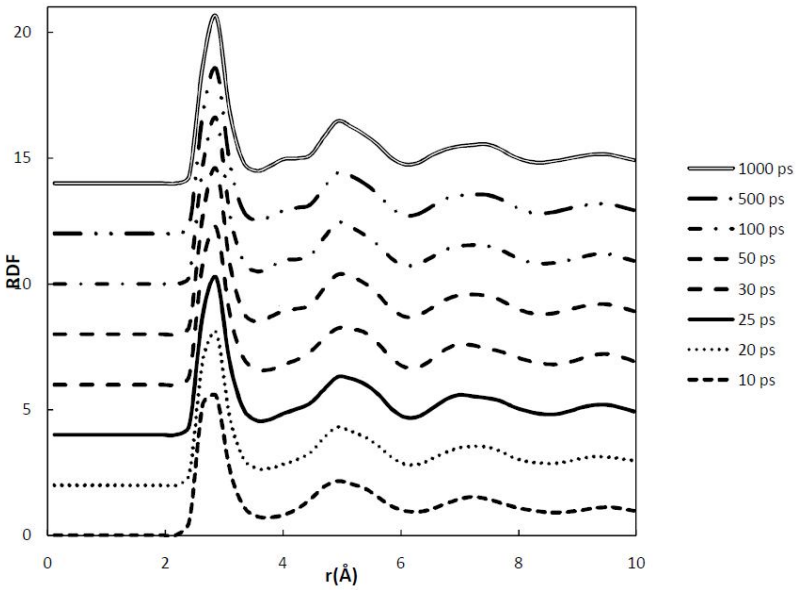

Fig. 6. Effect of relaxation time on RDF curve of rapidly solidified aluminum melt at 300 K. The melt was cooled at 10^{14} K/s

To study the dynamics of the system, the mean square displacement (MSD) of the aluminum atoms during solidification is shown in Fig. 7. As temperature decreases, the slope of the MSD curves decreases, which indicates the reduction of moving ranges of the atoms. Fig. 7a determines that MSD at a cooling rate of 10^{12} K/s was significantly higher than MSD at a cooling rate of 10^{13} K/s, indicating diffusion and rearrangements of the atoms at the lower cooling rates. It is evident that crystallization is accompanied by a wide range of atomic movements that results in significant change in the MSD curve. In contrast, at the high cooling rates, i.e. 10^{13} K/s and 10^{14} K/s, a metallic glass structure formed and thus MSD curves do not show much difference (Fig. 7b). In other words, when the system solidifies amorphously, atoms do not fluctuate in a wide range, i.e. they move within their neighborhood; hence, low MSD values are obtained. The results presented in Fig. 7 support the findings of internal energy and RDF curves: with increasing the heating rate from 10^{12} K/s to 10^{14} K/s, there was a tendency toward the formation of an amorphous-like structure.

Figure 8 shows the internal energy of the system as a function of temperature during the remelting process. The remelting temperature for the heating rate of 10^{12} K/s was in the range of 796-810 K, which was lower than that of the melting step. This is attributed to the initial structure of the material (partially crystalline) which affects the internal energy of the system. With increasing the heating rate to 10^{13} K/s, a plateau in the internal energy in the temperature range of 345 to 445 K was observed, while the remelting temperature shifted to 824-839 K (about 120 K lower than the melting stage). Figure 9 shows the variation of RDF during the remelting process at the rate of 10^{13} K/s. During heating, the degree of crystallinity progressively increased by increasing the temperature from 300 K to 400 K. In contrast to this observation, remelting with the heating rate of 10^{14} K/s was not accompanied by any crystallization. This observation shows the tendency of the structure to become crystalline if the heating rate is low enough to allow thermal-induced crystallization.

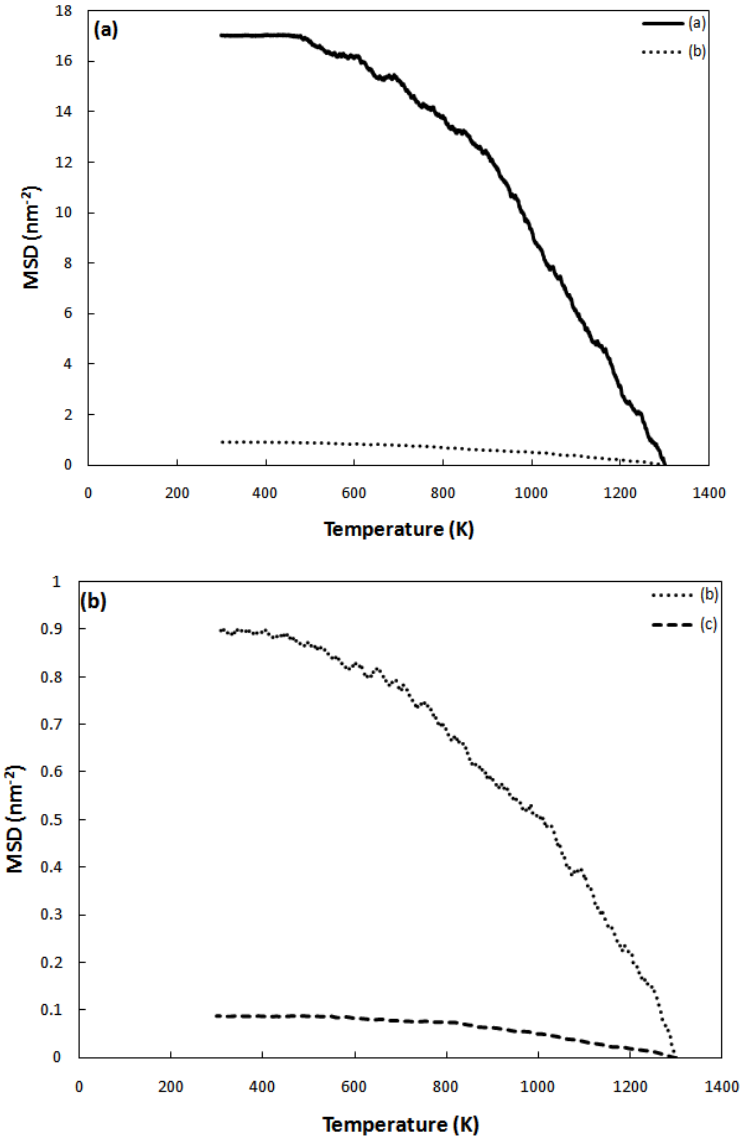

Fig. 7. MSD as a function of temperature for solidification of aluminum melt at three different cooling rates of (a) 10^{12} K/s, (b) 10^{13} K/s, and (c) 10^{14} K/s

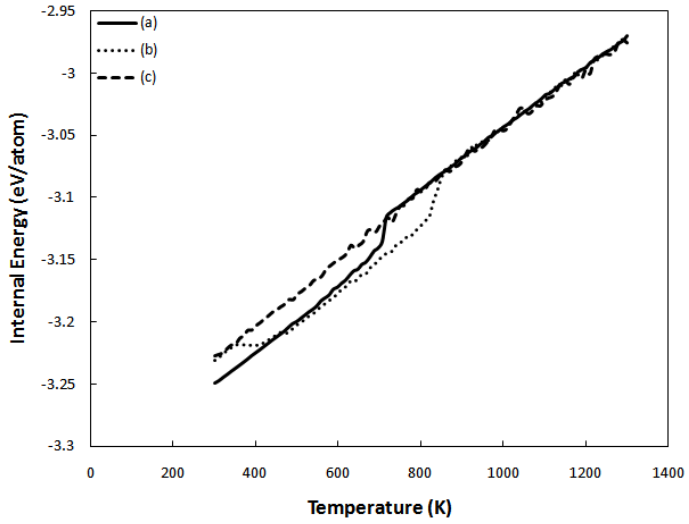

Fig. 8. Internal energy of the system during remelting: (a) 10^{12} K/s, (b) 10^{13} K/s and (c) 10^{14} K/s

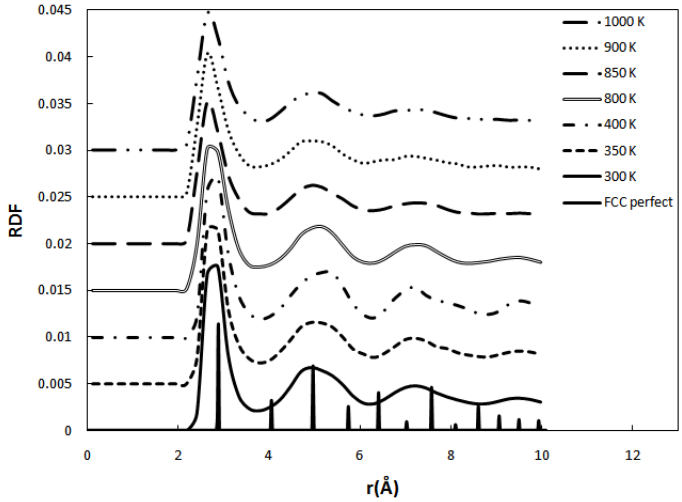

Fig. 9. RDF curves for aluminum during remelting process at a rate of 10^{13} K/s at some selected temperatures

As reported above, using the internal energy of the system as a function of temperature during cooling and heating of the system, a range of temperatures for melting and crystallization point can be achieved. In order to find the exact points of melting and crystallization another approach was established. Qi et al. [27] defined the melting temperature as the maximum value in the heat capacity. The comparison of the internal energy and C_v for the system during melting, solidification and remelting at a rate of 10^{13} K/s is shown in Fig. 10. As the results show, this method can also be used to investigate the temperature of crystallization which resulted in a negative value of C_v and indicated a reduction in internal energy. Based on this criterion, the effect of heating rate on the phase transformation temperature during melting, solidification and remelting for aluminum was identified (Table 3). Since no crystallization occurs at the rate of 10^{14} K/s, the glass transition temperature (T_g) was studied. For amorphous materials, the Wendt–Abraham parameter (g_{min}/g_{max}) [28] is commonly used to determine T_g; here, g_{min} and g_{max} are the first minimum and maximum values of RDF curves, respectively. Figure 11 shows the variation of Wendt–Abraham parameter as a function of temperature for solidification of aluminum at a rate of 10^{14} K/s. The results suggested a glass transition temperature of 735 K.

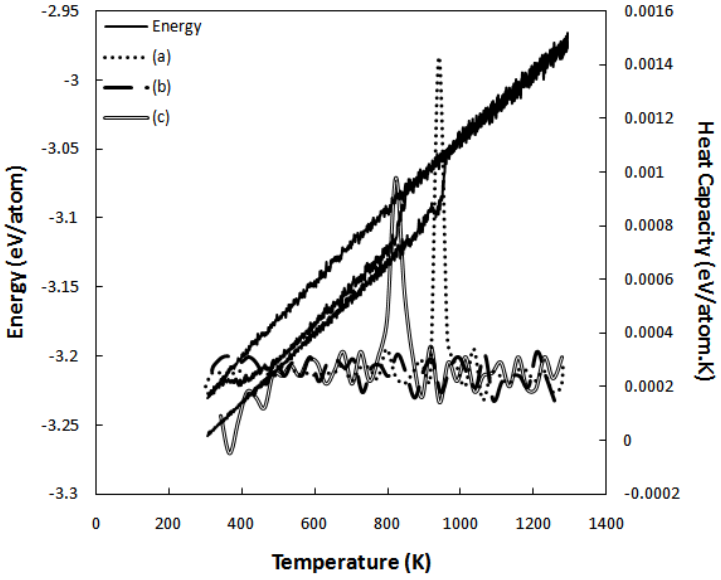

Fig. 10. Values of the heat capacity of aluminum as a function of temperature: (a) melting; (b) solidification; (c) remelting. The heating and cooling rates were 10^{13} K/s

Table 3. Phase transformation temperature (K) of aluminum obtained from the variation of heat capacity with temperature during melting, solidification and remelting processes

Rate (K/s)	Melting	Solidification	Remelting
10^{12}	896^{m}	462^{c}	691^{m}
10^{13}	941^{m}	-	365^{c} , 821^{m}
10^{14}	1135^{m}	-	-

m: melting, *c*: crystallization

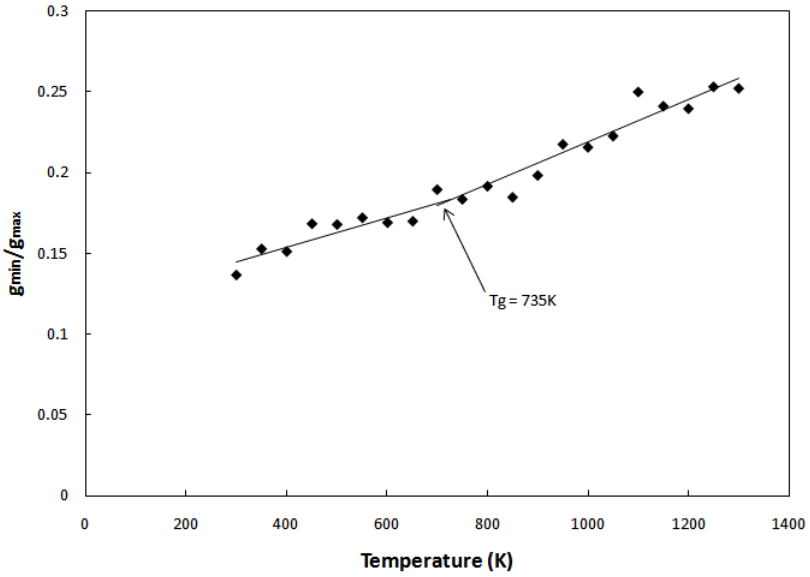

Fig. 11. Wendt–Abraham parameter for aluminum melt during solidification at the rate of 10^{14} K/s, showing the glass transition temperature at 735 K

4. CONCLUSION

Rapid melting, solidification and remelting of a system containing 500 aluminum atoms was investigated by a series of molecular dynamics simulations in NVT ensemble. The findings can be summarized as follows:

- The melting temperature of crystalline aluminum depends on the heating rate. The melting temperature increased from 896 K to 1135 K with increasing the heating rate from 10^{12} K/s to 10^{14} K/s.
- The melted aluminum atoms crystallized to FCC structure at 462 K during cooling with a rate of 10^{12} K/s. At higher cooling rates, however, amorphous-like structures formed.
- Calculating of the Wendt–Abraham parameter suggested a glass transition occurred at 735 K when the aluminum melt was rapidly cooled a rate of 10^{14} K/s.
- During remelting, the amorphous-like structure has higher internal energy, leading to a decrease in the melting temperature. The depletion of the melting temperature is estimated to be about 100 K and 120 K for the heating rates of 10^{12} K/s and 10^{13} K/s, respectively.
- During remelting of the rapidly solidified aluminum, the amorphous structure of the metal crystallized at around 365 K when a heating rate of 10^{13}K/s was employed. This phase transformation was found to be prohibited at a higher heating rate of 10^{14} K/s.

- The temperature of structural evolutions was determined using the values of heat capacity versus temperature.

REFERENCES

1. Liu, J., Zhao, J. Z.& Hu, Z. Q. (2007). The development of microstructure in a rapidly solidified Cu. *Materials Science and Engineering A*. pp. 452-453.
2. Dontsov, V. I. & Gogolin, V. P. (1996). Kinetic properties of metallic melts in the solidification interval. *Rasplavy*, pp. 107-111.
3. Hui, L. et al. (1998). Molecular dynamics simulation of structural changes of liquid fe3al. *Transactions of Nonferrous Metals Society of China (English Edition)*, Vol. 8, pp. 600-601.
4. Wang, L., Bian, X. & Li, H. (2000). Liquid-solid transition and crystal growth of metal Cu by molecular dynamics simulation. *Acta Physico - Chimica Sinica*, Vol. 16, p. 829.
5. Wang, L. et al. (2002). Atomic simulation of amorphization and crystallization of Ag50Au50 alloy during rapid solidification. *Transactions of Nonferrous Metals Society of China (English Edition)*, Vol. 12, pp. 845-849.
6. Wang, L., Yi, S. & Bian, X. F. (2002). Atom clusters in liquid and amorphous of Ni3Al alloy. *Acta Physico - Chimica Sinica*, Vol. 18, pp. 297-301.
7. Li, B. et al.(2004). Molecular dynamics simulations of the effects of defects on martensite nucleation. *Journal of Applied Physics*, Vol. 95, pp. 1698-1705.
8. Pei, Q. X., Lu, C. & Fu, M. W. (2004). The rapid solidification of Ti3Al: A molecular dynamics study. *Journal of Physics Condensed Matter*, Vol. 16, pp. 4203-4210.
9. Qi, L., Zhang, H. & Hu, Z. (2004). Molecular dynamic simulation of melting and solidification in binary liquid metal: Cu-Ag. *Jinshu Xuebao/Acta Metallurgica Sinica 40*, pp. 736-740.
10. Qi, L., Zhang, H. F. & Hu, Z. Q. (2004). Molecular dynamic simulation of glass formation in binary liquid metal: Cu-Ag using EAM. *Intermetallics*, Vol. 12, pp. 1191-1195.
11. Liu, J., Zhao, J. & Hu, Z. (2005). Molecular dynamic simulation of atomic clusters evolution in Cu-50%Ni alloy during rapid solidification. *Jinshu Xuebao/Acta Metallurgica Sinica*, Vol. 41, pp. 219-224.
12. Zhou, G. & Gao, Q. (2005). Molecular dynamics simulation of the solidification of liquid gold nanowires. *Solid State Communications*, Vol. 136, pp. 32-35.
13. Kart, S. Ö. et al. (2006). Molecular dynamics studies on glass formation of Pd-Ni alloys by rapid quenching. *Turkish Journal of Physics*, Vol. 30, pp. 319-327.
14. Kazanc, S. (2006). Molecular dynamics study of pressure effect on glass formation and the crystallization in liquid CuNi alloy. *Computational Materials Science*, Vol. 38, pp. 405-409.
15. Özdemir Kart, S., et al. (2006). Structural, thermodynamical, and transport properties of undercooled binary Pd-Ni alloys. *Materials Science and Engineering A*, pp. 435-436 and 736-744.
16. Guorong, Z. & Qiuming, G. (2007). Molecular dynamics simulation of the solidification of liquid nickel nanowires. *Diffusion and Defect Data Pt.B: Solid State Phenomena*, pp. 121-123 and 1053-1056.
17. Kazanc, S. (2007). Molecular dynamics study of pressure effect on crystallization behaviour of amorphous CuNi alloy during isothermal annealing. *Physics Letters, Section A: General, Atomic and Solid State Physics*, Vol. 365, pp. 473-477.
18. Kazanc, S. et al. (2007). Pressure effect on intermediate structures during transition from amorphous to crystalline states of copper. *Computational Materials Science 40*, pp. 179-185.
19. Liu, R. S., et al. (2007). Formation and magic number characteristics of cluster configurations during rapid cooling processes of liquid metals. *Diffusion and Defect Data Pt.B: Solid State Phenomena*, pp. 121-123 and 1139-1142.

20. Mendelev, M. I., et al. (2008). Analysis of semi-empirical interatomic potentials appropriate for simulation of crystalline and liquid Al and Cu. *Philosophical Magazine*, Vol. 88, 1723-1750.
21. Sarkar, A., Barat, P. & Mukherjee, P. (2008). Molecular dynamics simulation of rapid solidification of aluminum under pressure. *International Journal of Modern Physics B*, Vol. 22, pp. 2781-2785.
22. Tian, Z. A. et al., (2008), Molecular dynamics simulation for cooling rate dependence of solidification microstructures of silver. *Journal of Non-Crystalline Solids*, Vol. 354, pp. 3705-3712.
23. Berendsen, H. J. C. et al. (1984). Molecular dynamics with coupling to an external bath. *The Journal of Chemical Physics*, Vol. 81, pp. 3684-3690.
24. Swope, W. C., et al. (1982). A computer simulation method for the calculation of equilibrium constants for the formation of physical clusters of molecules: Application to small water clusters. *The Journal of Chemical Physics*, Vol. 76, pp. 637-649.
25. Sutton, A. P. & Chen, J. (1990). Long-range finnis–sinclair potentials. *Philosophical Magazine Letters*, Vol. 61, pp. 139-146.
26. Rafii-Tabar, H. & Chirazi, A. (2002). Multi-scale computational modelling of solidification phenomena. *Physics Report*, Vol. 365, pp. 145-249.
27. Qi, Y., et al. (2001). Melting and crystallization in Ni nanoclusters: The mesoscale regime. *Journal of Chemical Physics*, Vol. 115, pp. 385-394.
28. Wendt, H. R. & Abraham, F. F. (1978). Empirical criterion for the glass transition region based on Monte Carlo simulations. *Physical Review Letters*, Vol. 41, pp. 1244-1246.